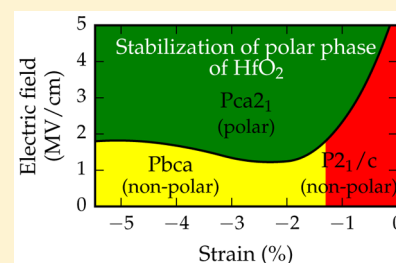


# Factors Favoring Ferroelectricity in Hafnia: A First-Principles Computational Study

Rohit Batra,<sup>†</sup> Tran Doan Huan,<sup>†</sup> Jacob L. Jones,<sup>‡</sup> George Rossetti, Jr.,<sup>†</sup> and Rampi Ramprasad<sup>\*,†</sup><sup>†</sup>Department of Materials Science & Engineering, University of Connecticut, Storrs, Connecticut 06269, United States<sup>‡</sup>Department of Materials Science and Engineering, North Carolina State University, Raleigh, North Carolina 27695, United States

## S Supporting Information

**ABSTRACT:** The surprising ferroelectricity displayed by hafnia thin films has been attributed to a metastable polar orthorhombic ( $Pca2_1$ ) phase. Nevertheless, the conditions under which this (or another competing) ferroelectric phase may be stabilized remain unresolved. It has been hypothesized that a variety of factors, including strain, grain size, electric field, impurities and dopants, may contribute to the observed ferroelectricity. Here, we use first-principles computations to examine the influence of mechanical and electrical boundary conditions (i.e., strain and electric field) on the relative stability of a variety of relevant nonpolar and polar phases of hafnia. We find that although strain or electric field, independently, do not lead to a ferroelectric phase, the combined influence of in-plane equibiaxial deformation and electric field results in the emergence of the polar  $Pca2_1$  structure as the equilibrium phase. The results provide insights for better controlling the ferroelectric characteristics of hafnia thin films by adjusting the growth conditions and electrical history.



## INTRODUCTION

Although hafnia is a well-known and well-studied high dielectric constant (“high- $k$ ”) material,<sup>1–7</sup> there has been renewed excitement about this material due to recent empirical observations of ferroelectricity in thin hafnia films, in both pure and doped forms.<sup>8–10</sup> These ferroelectric (FE) measurements along with excellent Si compatibility, easy complementary metal oxide semiconductor (CMOS) integration, and high scalability make hafnia a promising candidate for future nonvolatile memory applications over conventional perovskite-based materials.<sup>10</sup> However, these FE property observations are rather surprising since all the known equilibrium phases of hafnia, namely, the room temperature monoclinic (M)  $P2_1/c$  phase, the high temperature tetragonal (T)  $P4_2/nmc$  and cubic (C)  $Fm\bar{3}m$  phases, and the high-pressure orthorhombic (OA)  $Pbca$  and (OB)  $Pnma$  phases, are centrosymmetric and hence nonpolar.<sup>11</sup> Grazing incidence and  $\theta$ - $2\theta$  X-ray diffraction investigations on these thin FE hafnia films have suggested the presence of a polar orthorhombic (P-O1)  $Pca2_1$  phase as the origin of this unexpected FE behavior.<sup>10</sup> In fact, Sang et al.<sup>12</sup> in a combined TEM and nanoscale electron diffraction study were able to identify the polar P-O1 phase in a FE hafnia film. However, remarkable structural similarity between different phases of hafnia, especially the P-O1 and the OA phases, and limited statistics owing to the small film thicknesses (<20 nm) lead to some degree of uncertainty in these conclusions.

Several first-principles theoretical studies have also complemented these experimental findings.<sup>13–16</sup> The energy difference between the P-O1 and the known equilibrium phases of hafnia has been predicted to be small over wide temperature and pressure ranges.<sup>13</sup> Additionally, another

competing, though higher in energy, polar orthorhombic (P-O2)  $Pmn2_1$  phase has also been suggested as a potential phase responsible for the observed FE behavior. More importantly, a shallow kinetic energy barrier between the T and the aforementioned polar phases was also reported, suggesting their possible formation from the T phase. The fact that all FE thin films of hafnia have been reported to contain some volume fraction of the T phase<sup>17</sup> makes this finding even more intriguing with respect to the formation pathway of the FE phase(s). Figure 1 portrays the low-energy M, T, OA, P-O1, and P-O2 phases discussed above, for unit cells oriented in an equivalent manner. The equivalent orientations of different phases are discussed in later sections.

Besides identifying the potential FE phase(s) in hafnia films, many efforts, both empirical and theoretical, have been made to determine extrinsic factors which may stabilize a polar phase. Among various factors, the grain size is undoubtedly a critical one.<sup>10</sup> Almost all studies on FE hafnia films have demonstrated a monotonic decrease in the spontaneous polarization of films with increasing film thickness, which is proportional to the hafnia grain size. A critical grain size of  $\sim 20$  nm was identified above which the FE behavior eventually disappears.<sup>10</sup> The increasing volume fraction of M phase with increasing film thickness (or grain size) was ascribed as the reason for this observation. Although finite size effects are known to stabilize the nonpolar T phase in hafnia (and its twin oxide, zirconia) at small length scales,<sup>15,18</sup> we have suggested in the past that surface orientations and grain size may lead to a stabilization of

Received: November 28, 2016

Revised: January 23, 2017

Published: February 2, 2017

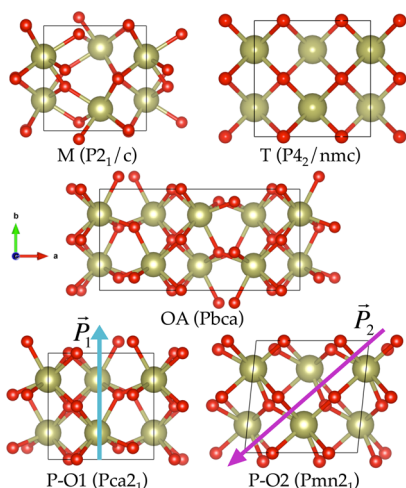


**Figure 1.** The (001) projections of the low-energy phases of hafnia. The polarization directions of the two polar phase are represented by  $\vec{P}_1$  and  $\vec{P}_2$ . Hf and O atoms are shown in green and red colors, respectively.

the P-O2 or the T phase in hafnia.<sup>14</sup> Observations of distinct FE behavior in pure hafnia thin films (6–10 nm) further strengthen the notion that surface energy plays a vital role in the stabilization of the FE phase.<sup>19</sup> Furthermore, on the basis of a phenomenological model of the surface energies of different polymorphs of hafnia, Materlik et al.<sup>20</sup> were able to explain the origins of ferroelectricity and antiferroelectricity in HfZrO<sub>2</sub> and ZrO<sub>2</sub> thin films, respectively.

Another important factor is the residual stresses in these films. One source of stress is from the mechanical barrier provided by the capping of the top and the bottom electrodes during crystallization of the films. Additionally, there is an anisotropic stress introduced due to the lattice and thermal coefficient mismatch between the film and the substrate. Studies from Kisi et al.<sup>21</sup> and Park et al.<sup>22</sup> have suggested the possibility of the T to P-O1 transformation due to in-plane compressive and out-of-plane tensile stresses in the (*a*, *b*) plane and along the *c*-direction, respectively, of the T phase.

Observations of antiferroelectricity, the “wake-up effect”, and “fatigue” behavior in hafnia films have also insinuated the possibility of electric field induced stabilization of the hafnia FE phases.<sup>17,23</sup> Particularly interesting, and relevant to this work, is the “wake-up effect”. This term was coined to describe the phenomenon of improving (and/or inducing) FE loops of hafnia films, which displayed no apparent ferroelectricity in their pristine form, through electric field cycling. Dopants present in these films are yet another important factor.<sup>10</sup> While it is generally agreed upon that their presence enhances the thermodynamic window to stabilize the FE phase, whether they have any principal role in the appearance of the FE phase remains uncertain. Although thermal effects are known to stabilize the tetragonal and the cubic phases of hafnia at high temperatures of ~2000 and ~2800 K,<sup>11</sup> they are not expected to have a significant role at room temperatures at which these ferroelectric measurements are made.

From the previous discussion, one may conclude that the important factors responsible for FE behavior in hafnia films are (1) surface energy due to the small grain sizes, (2) nonhydrostatic stresses associated with the electrodes and the substrate, (3) applied electric field, and (4) dopants. The surface energy factor has been studied extensively in past

works.<sup>14,20</sup> In the present paper, we focus exclusively on the second and the third factors, namely, the role of stresses and electric field. We employ first-principles density functional theory (DFT) calculations to determine the effects of these factors, independently as well as in combination, and find the thermodynamic conditions under which a polar phase becomes favored in bulk hafnia. First, we compare the relative stabilities of different phases of hafnia under hydrostatic pressures. Next, we study their relative stability under biaxial deformations, which resemble the physical conditions expected to be present in thin films due to thermal expansion coefficient and lattice mismatch with the substrate. Our calculations suggest that under compressive stresses both the P-O1 and the OA phases become stable relative to the M phase. While the nonpolar OA phase was found to exhibit the lowest energy under such conditions, it was closely followed by the P-O1 phase. We further found that electric field oriented along the polarization direction of the two polar phases significantly reduces their relative energies with respect to the M phase. Nonetheless, the M phase remains the equilibrium phase under electric field as high as 5 MV/cm.

Thus, independently, neither the biaxial deformations nor the electric field was found to stabilize a polar phase in bulk hafnia. However, under the *combined* effect of compressive stresses and electric field, the polar P-O1 phase was found to become the equilibrium phase. These results provide a possible pathway for the observation of FE behavior in hafnia films due to the presence of the P-O1 phase, especially given the observation of the “wake-up effect”. In light of the previously suggested pathway for the formation of polar phase(s) from the T phase stabilized due to surface energy effects, we make a special note here that the present results provide an additional route for the stabilization of a polar phase in hafnia. It is possible that depending on the prevailing factors in hafnia films, both the routes are accessed, leading to the formation of a FE phase.

## THEORETICAL METHODS

Electronic structure DFT calculations were performed to obtain the relative energies of different phases of bulk hafnia under equilibrium, hydrostatic pressure, and biaxially deformed conditions. In this study, we considered the following five different phases of hafnia—M, T, OA, P-O1, and P-O2—as these were either empirically observed or were theoretically predicted to have low energy under the thermodynamic conditions relevant in FE hafnia thin films. The DFT calculations were performed using the Vienna *Ab Initio* Simulation Package<sup>24</sup> (VASP) employing the Perdew–Burke–Ernzerhof exchange–correlation functional<sup>25</sup> and the projector-augmented wave methodology.<sup>26</sup> A  $6 \times 6 \times 6$  Monkhorst–Pack mesh<sup>27</sup> for *k*-point sampling and a basis set of plane waves with kinetic energies up to 500 eV were used to represent the wave functions. Equivalent four hafnia-unit supercells, constructed using the parameters obtained from ref 13, were first relaxed to obtain the equilibrium lattice parameters of the aforementioned phases. Equibiaxial deformations along the [100] and [010] directions were then introduced in these phases to simulate in-plane compressive and tensile stresses. The deformations were introduced by rescaling the lattice vectors of a phase while maintaining the relative coordinates of its constituent atoms. While all atoms in the deformed structure were allowed to relax until atomic forces were smaller than  $10^{-2}$  eV/Å, the simulation cell was allowed to relax only along the [001] direction (i.e., the *c*-axis),

**Table 1.** Lattice Parameters and the Spontaneous Polarization of Reoriented Equivalent Supercells of the Five Phases of Hafnia<sup>a</sup>

phase	<i>a</i> (Å)	<i>b</i> (Å)	<i>c</i> (Å)	$\beta$ (deg)	$\gamma$ (deg)	<i>V</i> (Å <sup>3</sup> /HfO <sub>2</sub> )	<i>P</i> (μC/cm <sup>2</sup> )
M	5.15 (5.14, <sup>b</sup> 5.12 <sup>c</sup> )	5.20 (5.20, <sup>b</sup> 5.17 <sup>c</sup> )	5.33 (5.31, <sup>b</sup> 5.29 <sup>c</sup> )	99.7 (99.8, <sup>b</sup> 99.2 <sup>c</sup> )	90 (90, <sup>b</sup> 90 <sup>c</sup> )	35.15	0 (0 <sup>b</sup> )
T	5.08 (5.08, <sup>b</sup> 5.08 <sup>d</sup> )	5.08 (5.08, <sup>b</sup> 5.08 <sup>d</sup> )	5.23 (5.28, <sup>b</sup> 5.20 <sup>d</sup> )	90 (90, <sup>b</sup> 90 <sup>d</sup> )	90 (90, <sup>b</sup> 90 <sup>d</sup> )	33.78	0 (0 <sup>b</sup> )
P-O1	5.06 (5.01, <sup>b</sup> 4.90 <sup>d</sup> )	5.09 (5.08, <sup>b</sup> 4.92 <sup>d</sup> )	5.27 (5.29, <sup>b</sup> 5.10 <sup>d</sup> )	90 (90, <sup>b</sup> 90 <sup>d</sup> )	90 (90, <sup>b</sup> 90 <sup>d</sup> )	33.90	50 (52 <sup>b</sup> )
P-O2	5.13 (5.12 <sup>b</sup> )	5.13 (5.12 <sup>b</sup> )	5.18 (5.18 <sup>b</sup> )	90 (90 <sup>b</sup> )	84.07 (83.51 <sup>b</sup> )	33.90	56 (56 <sup>b</sup> )
OA	10.07/2 = 5.03 (10.03, <sup>b</sup> 10.02 <sup>c</sup> )	5.09 (5.08, <sup>b</sup> 5.06 <sup>c</sup> )	5.25 (5.27, <sup>b</sup> 5.23 <sup>c</sup> )	90 (90, <sup>b</sup> 90 <sup>c</sup> )	90 (90, <sup>b</sup> 90 <sup>c</sup> )	33.64	0 (0 <sup>b</sup> )

<sup>a</sup>Unit cells containing four HfO<sub>2</sub> formula units of the different phases were reoriented such that their *a*- and *c*-axes correspond to the smallest and the largest crystallographic axes, respectively. For example, the *a*- and *b*-axes of the standard P-O1 phase were reoriented as *c*- and *a*-axes, respectively. The findings of the past studies (within parentheses) have also been modified appropriately for comparison. <sup>b</sup>Reference 13. <sup>c</sup>Reference 31. <sup>d</sup>Reference 32. <sup>e</sup>Reference 33.

thus resulting in an in-plane stress condition. Such constrained relaxation produced a uniform deformation of the cell and thus allowed us to simulate in-plane stresses while preserving the space group symmetry of a phase. Further remarks rationalizing the restriction to equibiaxial deformations to model anisotropic stresses will be made in later sections.

In order to understand the impact of electric field on the phase stability of hafnia, energies of different phases under the influence of an electric field were also computed. The energy of a phase  $\alpha$  with volume  $V_0^\alpha$  and under an electric field  $\vec{E}$  was calculated using the expression<sup>28</sup>

$$E^\alpha = E_{\text{DFT}}^\alpha - V_0^\alpha (\epsilon_r^\alpha \epsilon_0 \vec{E} + \vec{P}^\alpha) \vec{E} \quad (1)$$

where  $E_{\text{DFT}}^\alpha$  is the DFT computed energy,  $\vec{P}^\alpha$  and  $\epsilon_r^\alpha$  are the spontaneous polarization and matrix representation of the relative permittivity of the phase  $\alpha$ , respectively, and  $\epsilon_0$  is the permittivity of vacuum. Since  $\vec{E}$  is a vectorial quantity, its effect is dependent on its magnitude as well as direction. From eq 1 it is evident that the effect of electric field on the energy of a phase is maximized when the dot product  $\vec{P}^\alpha \cdot \vec{E}$  is maximum, i.e., when the electric field is oriented parallel to the polarization direction of a polar phase. Thus, two important orientations of electric field—parallel to the polarization vectors  $\vec{P}_1$  and  $\vec{P}_2$  of the polar phases P-O1 and P-O2, respectively (see Figure 1)—were studied in this work. Further, for each orientation, we consider the phase stability under three different states, i.e., the stress-free, the hydrostatic, and the in-plane stress states. The density functional perturbation theory and the Berry phase evaluation were respectively employed to obtain the relative permittivity matrix and the spontaneous polarization of the different phases of hafnia. Spontaneous polarization computations were repeated using the ABINIT<sup>29</sup> package to further verify the VASP computed values.

## RESULTS AND DISCUSSION

### Hydrostatic Pressures and Equibiaxial Deformations.

Table 1 lists the lattice parameters of the five phases of hafnia, as predicted from our DFT computations. We make a note that the reported cell parameters of each phase are chosen such that minimal cell strains and atom shuffles reduce a phase to the four formula unit T phase (see caption of Table 1). An excellent agreement between the findings of this work and the past studies is apparent from the table. One comment about the choice of density functional should be made in reference to the

hafnia system. Although both the LDA and the GGA density functionals produce the same energy ordering of different phases of hafnia, LDA functionals have been shown to consistently result in smaller relative energies between different polymorphs of hafnia in comparison to that of the GGA predicted values.<sup>20,30</sup> Nevertheless, these relative energies are substantial and the choice of density functional is not expected to cause any major changes to the conclusions of this work.

Simply by looking at the volume of these phases, one can make a direct inference that compressive stresses and lower volumes may stabilize other phases of hafnia over the M phase. This observation, along with the empirical suggestions of the critical role of anisotropic residual stresses arising from interactions with electrode capping layers and/or the substrate in the FE hafnia films, forms the basis for studying the phase stability of hafnia under hydrostatic and anisotropic stresses. One important comment about the expected anisotropic stresses in hafnia films should be made. Generally, thin films are known to have biaxial stresses in the plane parallel to the film–substrate interface. However, in the case of hafnia films the situation is more complicated due to the additional mechanical stress from the top and bottom electrode capping along the direction normal to the film. Thus, hafnia films are exposed to anisotropic stresses of varying magnitude in all three directions, leaving us with a formidable modeling challenge to study numerous possible stress profiles. In addition to this, the stresses (or strains) experienced by different phases in a film will also be dissimilar and would depend on their respective lattice parameter misfits. Thus, instead of making an attempt to model the myriads of complicated conditions precisely, we aim to gain qualitative insights about the role played by the anisotropic stresses in hafnia films by studying bulk hafnia under two rather simple, yet informative and representative, scenarios: (1) hydrostatic pressures and (2) equibiaxial deformations. While hydrostatic pressures allow us to predict the most stable phase at fixed volume (approximately simulating out-of-plane mechanical barrier from electrodes and in-plane stresses from substrate), equibiaxial deformations help us compare energies of phases at fixed in-plane area (effectively mimicking the role of a substrate). Another reason for restricting the computations to equibiaxial deformations is that such deformations help preserve the symmetry of the phases involved. Further, we consider deformations only in the (001) plane, as significant effects of equibiaxial deformations

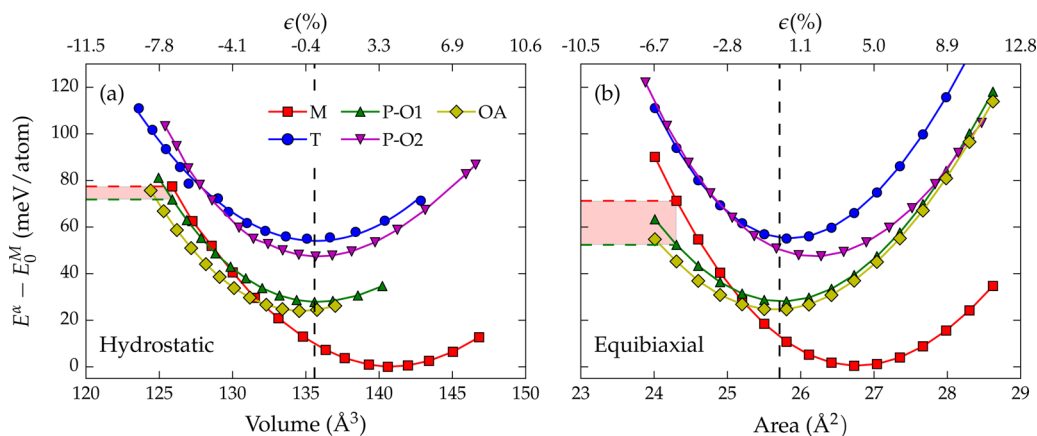


**Figure 2.** Energy variation of different phases of hafnia under (a) hydrostatic pressure and (b) equibiaxial deformation, referenced to the energy of the equilibrium bulk M phase. Percentage strain are reported in reference to the equilibrium P-O1 phase.

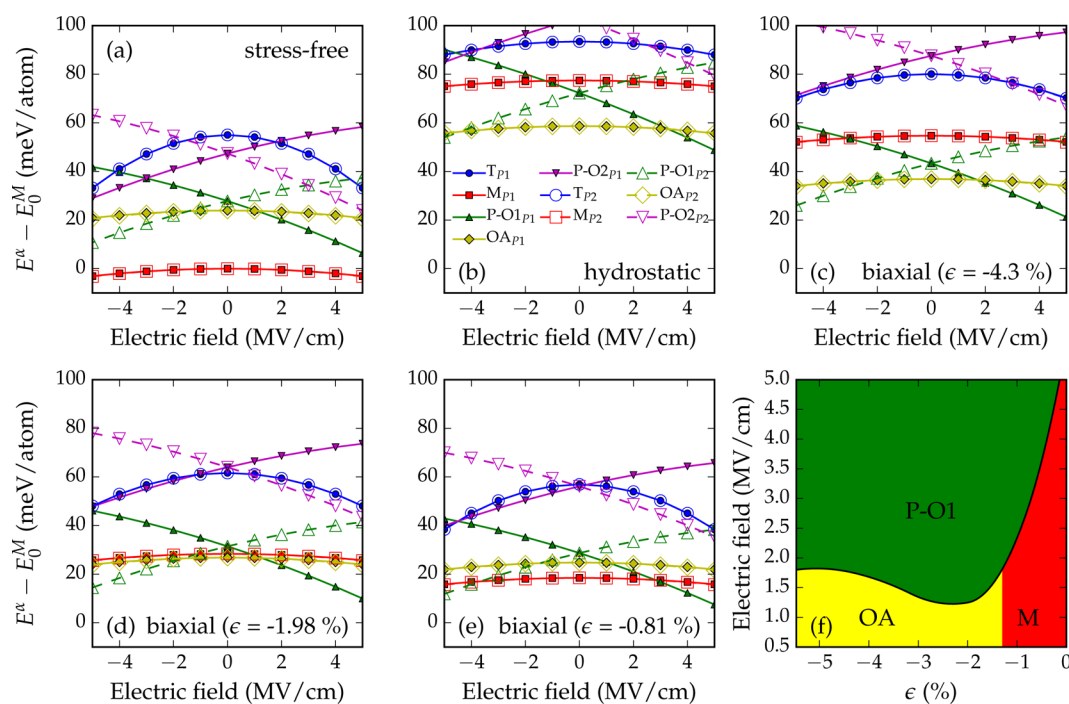


**Figure 3.** Influence of electric field on the free energy (using eq 1) of different phases of hafnia under (a) stress-free, (b) hydrostatic compression, and in-plane compressive stress states corresponding to strain (in reference to the equilibrium P-O1 phase) of (c) 4.3%, (d) 1.98%, and (e) 0.81%. Results for two special orientations of electric field, parallel to the polarization directions  $\bar{P}_1$  (solid symbols) and  $\bar{P}_2$  (open symbols) of the P-O1 and the P-O2 phases, respectively, are presented. The free energy of the 0 K bulk M phase is set to zero. Panel (f) represents the computed phase diagram of hafnia under the influence of electric field and in-plane stresses. The green, red, and yellow colors signify regions where the P-O1, the M, and the OA phase, respectively, are the ground state. Electric fields above about 4 MV/cm are unrealistically high and may not be physically realizable without adversely damaging the material.

are expected to be observed in this direction due to large differences between the (*a*, *b*) lattice parameters of the M phase compared to those of the other phases.

We first discuss the results of phase stability in hafnia under hydrostatic compression and tension. From Figure 2a it is evident that at higher volumes the M phase is lowest in energy and corresponds to the equilibrium phase at 0 K. However, under a state of compression, i.e., at lower volumes, the high-pressure OA phase has the lowest energy and becomes the most stable phase, in agreement with the experimental phase diagram<sup>11</sup> and several computational studies.<sup>13,20,30</sup> Interestingly, the P-O1 phase also becomes stable relative to the M phase at lower volumes, although it is always higher in energy

than the equilibrium OA phase in this region. A remarkable similarity between the energy variation of the OA and the P-O1 phase is also evident and can be ascribed to the high degree of structural similarity between the two phases.

Next, we discuss the results of equibiaxial deformations presented in Figure 2b. Here we compare the relative stability of the phases as a function of the (001) planar area, i.e., adopting an approach analogous to that utilized when changing volume in the case of hydrostatic pressures. Similar trends in phase stability, as obtained under hydrostatic pressures, can be observed here as well with the OA phase stabilizing under compressive stresses. However, a noteworthy distinction between the two cases should be made. The stability of the

P-O1 phase, relative to the M phase, is significantly larger under the state of equibiaxial compression as compared to that of the hydrostatic compression. This is graphically illustrated in Figure 2 by the difference in the height of the shaded region for the two cases. Furthermore, the energy difference between the P-O1 and the OA phases is smaller under equibiaxial stress state as compared to that under hydrostatic compression state. Nonetheless, the results show no evidence of stabilization of a FE phase under both the hydrostatic and biaxially deformed stress-state scenarios considered here.

**Electric Field.** As discussed earlier, several empirical observations of a “wake-up effect” have been encountered in FE hafnia films.<sup>23,34–36</sup> Electric field induced phase transformation<sup>37</sup> is one proposed explanation for this behavior. Figure 3a presents the effect of electric field on the phase stability of hafnia using eq 1. Two special orientations of electric field, i.e., parallel to the direction of spontaneous polarization of the two polar phases, were considered. This allows us to estimate the maximum influence the electric field could have on the phase stability in hafnia. Here, the computations are restricted to an electric field with magnitude smaller than 5 MV/cm to be consistent with electric field range explored experimentally. Assuming orientational independence of dielectric response in the case of nonpolar phases, the second term on right side of eq 1 can be reduced to  $-V_0^\alpha(\bar{\epsilon}_r^\alpha)\epsilon_0|\vec{E}|^2$ , where  $\bar{\epsilon}_r^\alpha$  represents the average of the trace of the dielectric tensor,  $\epsilon_r^\alpha$ . This term represents the effect of induced polarization on the free energy, is always negative, and varies parabolically with the applied electric field  $\vec{E}$ . Thus, among the nonpolar phases, the phase with highest relative permittivity ( $\epsilon_r^\alpha$ ), i.e., the T phase, shows maximum parabolic change in the free energy with the applied electric field. In the case of polar phases, however, the dot product  $-V_0^\alpha\vec{P}\cdot\vec{E}$  forms the dominant term, particularly when the electric field is oriented parallel to the direction of spontaneous polarization of a polar phase. Thus, one can observe significant stabilization (destabilization) of the P-O1 or the P-O2 phase, relative to the M phase, when the applied electric field is oriented parallel (opposite) to the direction of polarization. We also note that the polarization directions of the two polar phases subtend an angle of 138°, leading to  $\vec{P}\cdot\vec{E}$  terms with opposite signs and thus contrary changes in the free energy. From Figure 3a we conclude that electric field (<5 MV/cm) cannot stabilize any of the two metastable polar phases in bulk hafnia; however, it can significantly reduce their energies closer to the equilibrium M phase, especially in the case of the P-O1 phase.

Given this observation, one may reasonably suppose that under the combined effect of electric field and other relevant factors, such as stress, dopants, oxygen vacancies, etc., pervasive in hafnia films, the P-O1 phase becomes the most stable phase. Particularly, the factors that destabilize the M phase can be expected to produce such conditions. On the basis of our previous findings, we already know that compressive stress (hydrostatic or in-plane) is one such factor that stabilizes OA and P-O1 phase relative to the M phase. Thus, we consider next the combined effect of compressive stresses and electric field on the phase stability of hafnia.

Panels b and c of Figure 3 present the variation of free energy of hydrostatically compressed (with volume  $\sim 126 \text{ \AA}^3$ ) and equibiaxially deformed (along the (001) plane with  $a, b = 4.96 \text{ \AA}$ ) phases of hafnia. For ease of comparison with Figure 3a, we set the energy of the bulk M phase as the reference energy.

Three important observations should be made in Figure 3b,c: (1) at  $|\vec{E}| = 0$ , all the phases increase in energy corresponding to the elastic energy associated with the deformations, (2) the P-O1 phase becomes the stable phase at large magnitude of electric field, with the smallest value being  $\sim 2 \text{ MV/cm}$ , which is around the same magnitude at which many empirical observations of the “wake-up effect” have been noticed,<sup>23</sup> and (3) the P-O1 phase stabilizes at lower magnitude of electric field in the case of equibiaxial deformations as compared to that of the hydrostatic pressures. It should be noted that owing to extrinsic breakdown of the hafnia films, it may be difficult to achieve electric fields of magnitude around 4 MV/cm in these films. This makes it challenging to stabilize the P-O1 phase in hafnia under hydrostatic compression through electric field. Furthermore, we note that owing to the symmetry of  $\epsilon_r^\alpha$  for the two electric field orientations considered here, the term  $V_0^\alpha(\epsilon_r^\alpha\epsilon_0\vec{E})\cdot\vec{E}$  in eq 1 has almost similar influence on energy of the phases for the two orientations. Thus, energies of nonpolar phases appear to overlap for the two orientations of electric field.

The above results raise an important question; i.e., can the P-O1 phase of hafnia become stable at realistic values of electric field and strain? To address this question, we plot in Figure 3f the interpolated “phase” diagram of bulk hafnia under the influence of electric field and (001) in-plane stress. At zero strain, the electric field required to stabilize the polar P-O1 phase is unrealistically high (consistent with Figure 3a). Interestingly, in Figure 3f, one can observe a dip in the magnitude of electric field required to stabilize the P-O1 phase at  $\sim 2\%$  compressive strain. This can be understood as follows. At lower compressive strains (0–1%), the electric field switches the ground state between the M and the P-O1 phase (see Figure 3e). Thus, at the lower strain levels, the phase boundary between the P-O1 and the M phase is determined by the rate of change of the relative energies of the M and the P-O1 phase, which can be observed to be high from Figure 2b. In contrast, at larger compressive strains (>2%), the electric field switches the ground state between the OA and the P-O1 phase (see Figure 3c,d). Thus, for larger strains (>2%), the phase boundary between the OA and the P-O1 phase is determined by the rate of change of the relative energies of the OA and the P-O1 phase. Overall, from Figure 3f one can conclude that there exists a region of realistic electric fields and strains which can favor stabilization of the polar P-O1 phase in hafnia.

The above results clearly suggest a pathway to induce ferroelectricity in hafnia through stabilization of the P-O1 phase owing to combined effect of electric field and compressive stresses. Although limited possibilities of stresses and electric field orientations were explored in this study, similar results can be expected for other combinations as well. This is because the equilibrium lattice parameters of the M phase are systematically larger than that of the other phases across all directions. We note that the simple modeling scheme adopted here is not adequate to represent/simulate the complex mechanical boundary constraints prevailing in hafnia films, and results obtained here cannot be directly extrapolated to real hafnia films. Nevertheless, the qualitative insights gained from this study on the possible role played by compressive stresses and electric field can serve as rational guidance toward synthesis of polar hafnia films. An important implication of this study is that a combination of factors operating simultaneously may be responsible for stabilizing the FE phases in hafnia films. While one factor (such as stress, surface energy, dopants, etc.) may

destabilize the equilibrium M phase, the other (such as electric field) may favor the FE phase, thus cumulatively resulting in stabilization of a FE phase. Therefore, it maybe worthwhile, though complex, to study the cumulative effect of surface energy, stresses, electric field, and defects on the phase stability in hafnia to develop a comprehensive understanding of the interaction or cooperation of these phenomena.

## CONCLUSIONS

In summary, we explored the independent as well as the combined influence of mechanical and electrical boundary conditions toward stabilization of a FE phase in hafnia. Two variants of mechanical boundary conditions; i.e., hydrostatic and in-plane stress states were examined. While hydrostatic compressive stresses were shown to stabilize the high pressure orthorhombic (*Pbca*) phase, in agreement with the empirical phase diagram of bulk hafnia, an even more significant finding of this work is that compressive stresses, both hydrostatic and in-plane, stabilize the polar orthorhombic (*Pca2<sub>1</sub>*) phase of hafnia with respect to the equilibrium monoclinic phase. In fact, in-plane compressive stresses, which are particularly relevant in thin films, stabilize this polar phase relatively more than the hydrostatic pressures.

Two variants of electrical conditions, with an applied electric field parallel to the polarization directions of the polar *Pca2<sub>1</sub>* and *Pmn2<sub>1</sub>* phase of hafnia, were also studied. They too were found to significantly reduce the relative energies of the two polar phases of hafnia. However, neither the mechanical nor the electrical boundary conditions *independently* lead to the stabilization of a FE phase of hafnia as the equilibrium phase.

Nonetheless, under the *combined* influence of compressive stresses and electric field, we found that the polar *Pca2<sub>1</sub>* phase can, indeed, become the equilibrium phase in bulk hafnia. Interestingly, the predicted magnitude of electric field at which this polar phase becomes stable falls well within the empirical range wherein the “wake-up effect” has been observed in hafnia films. These findings not only suggest compressive stresses and electric field as possible control parameters to better tune the FE characteristics of hafnia films, but more importantly, they show that multiple factors, operating in concert, may be responsible for the formation of the ferroelectric phase in hafnia films.

## ASSOCIATED CONTENT

### Supporting Information

The Supporting Information is available free of charge on the ACS Publications website at DOI: 10.1021/acs.jpcc.6b11972.

Data on relative permittivity and the spontaneous polarization of different phases of hafnia used to construct Figure 3 (PDF)

## AUTHOR INFORMATION

### Corresponding Author

\*E-mail: rampi.ramprasad@uconn.edu (R.R.).

### ORCID

Rohit Batra: 0000-0002-1098-7035

### Notes

The authors declare no competing financial interest.

## ACKNOWLEDGMENTS

Financial support of this work through Grant No. W911NF-15-1-0593 from the Army Research Office (ARO) and partial computational support through a Extreme Science and Engineering Discovery Environment (XSEDE) allocation number TG-DMR080058N are acknowledged.

## REFERENCES

- (1) Robertson, J. High dielectric constant gate oxides for metal oxide Si transistors. *Rep. Prog. Phys.* **2006**, *69*, 327.
- (2) Wilk, G. D.; Wallace, R. M.; Anthony, J. M. High- $\kappa$  gate dielectrics: Current status and materials properties considerations. *J. Appl. Phys.* **2001**, *89*, 5243–5275.
- (3) Zhu, H.; Tang, C.; Fonseca, L. R. C.; Ramprasad, R. Recent progress in ab initio simulations of hafnia-based gate stacks. *J. Mater. Sci.* **2012**, *47*, 7399–7416.
- (4) Zhu, H.; Ramanath, G.; Ramprasad, R. Interface engineering through atomic dopants in HfO<sub>2</sub>-based gate stacks. *J. Appl. Phys.* **2013**, *114*, 114310.
- (5) Shi, N.; Ramprasad, R. Local dielectric permittivity of HfO<sub>2</sub> based slabs and stacks: A first principles study. *Appl. Phys. Lett.* **2007**, *91*, 242906.
- (6) Tang, C.; Ramprasad, R. Oxygen defect accumulation at Si:HfO<sub>2</sub> interfaces. *Appl. Phys. Lett.* **2008**, *92*, 182908.
- (7) Ramprasad, R.; Shi, N. Dielectric properties of nanoscale HfO<sub>2</sub> slabs. *Phys. Rev. B: Condens. Matter Mater. Phys.* **2005**, *72*, 052107.
- (8) Börscke, T. S.; Müller, J.; Bräuhäus, D.; Schröder, U.; Böttger, U. Ferroelectricity in hafnium oxide thin films. *Appl. Phys. Lett.* **2011**, *99*, 102903.
- (9) Schroeder, U.; Yurchuk, E.; Müller, J.; Martin, D.; Schenk, T.; Polakowski, P.; Adelman, C.; Popovici, M. I.; Kalinin, S. V.; Mikolajick, T. Impact of different dopants on the switching properties of ferroelectric hafnium oxide. *Jpn. J. Appl. Phys.* **2014**, *53*, 08LE02.
- (10) Park, M. H.; Lee, Y. H.; Kim, H. J.; Kim, Y. J.; Moon, T.; Kim, K. D.; Müller, J.; Kersch, A.; Schroeder, U.; Mikolajick, T.; et al. Ferroelectricity and antiferroelectricity of doped thin HfO<sub>2</sub>-based films. *Adv. Mater.* **2015**, *27*, 1811–1831.
- (11) Ohtaka, O.; Fukui, H.; Kunisada, T.; Fujisawa, T.; Funakoshi, K.; Utsumi, W.; Irifune, T.; Kuroda, K.; Kikegawa, T. Phase relations and volume changes of hafnia under high pressure and high temperature. *J. Am. Ceram. Soc.* **2001**, *84*, 1369–1373.
- (12) Sang, X.; Grimley, E. D.; Schenk, T.; Schroeder, U.; LeBeau, J. M. On the structural origins of ferroelectricity in HfO<sub>2</sub> thin films. *Appl. Phys. Lett.* **2015**, *106*, 162905.
- (13) Huan, T. D.; Sharma, V.; Rossetti, G. A.; Ramprasad, R. Pathways towards ferroelectricity in hafnia. *Phys. Rev. B: Condens. Matter Mater. Phys.* **2014**, *90*, 064111.
- (14) Batra, R.; Tran, H. D.; Ramprasad, R. Stabilization of metastable phases in hafnia owing to surface energy effects. *Appl. Phys. Lett.* **2016**, *108*, 172902.
- (15) Reyes-Lillo, S. E.; Garrity, K. F.; Rabe, K. M. Antiferroelectricity in thin-film ZrO<sub>2</sub> from first principles. *Phys. Rev. B: Condens. Matter Mater. Phys.* **2014**, *90*, 140103.
- (16) Lowther, J. E.; Dewhurst, J. K.; Leger, J. M.; Haines, J. Relative stability of ZrO<sub>2</sub> and HfO<sub>2</sub> structural phases. *Phys. Rev. B: Condens. Matter Mater. Phys.* **1999**, *60*, 14485–14488.
- (17) Grimley, E. D.; Schenk, T.; Sang, X.; Pešić, M.; Schroeder, U.; Mikolajick, T.; LeBeau, J. M. Structural changes underlying field-cycling phenomena in ferroelectric HfO<sub>2</sub> thin films. *Adv. Electron. Mater.* **2016**, *2*, 1600173.
- (18) Pitcher, M. W.; Ushakov, S. V.; Navrotsky, A.; Woodfield, B. F.; Li, G.; Boerio-Goates, J.; Tissue, B. M. Energy crossovers in nanocrystalline zirconia. *J. Am. Ceram. Soc.* **2005**, *88*, 160–167.
- (19) Polakowski, P.; Müller, J. Ferroelectricity in undoped hafnium oxide. *Appl. Phys. Lett.* **2015**, *106*, 232905.
- (20) Materlik, R.; Künneth, C.; Kersch, A. The origin of ferroelectricity in Hf<sub>1-x</sub>Zr<sub>x</sub>O<sub>2</sub>: A computational investigation and a surface energy model. *J. Appl. Phys.* **2015**, *117*, 134109.

- (21) Kisi, E. H.; Howard, C. J.; Hill, R. J. Crystal structure of orthorhombic zirconia in partially stabilized zirconia. *J. Am. Ceram. Soc.* **1989**, *72*, 1757–1760.
- (22) Hyuk Park, M.; Joon Kim, H.; Jin Kim, Y.; Moon, T.; Seong Hwang, C. The effects of crystallographic orientation and strain of thin Hf<sub>0.5</sub>Zr<sub>0.5</sub>O<sub>2</sub> film on its ferroelectricity. *Appl. Phys. Lett.* **2014**, *104*, 072901.
- (23) Schenk, T.; Yurchuk, E.; Mueller, S.; Schroeder, U.; Starschich, S.; Böttger, U.; Mikolajick, T. About the deformation of ferroelectric hystereses. *Appl. Phys. Rev.* **2014**, *1*, 041103.
- (24) Kresse, G.; Furthmüller, J. Efficient iterative schemes for *ab initio* total-energy calculations using a plane-wave basis set. *Phys. Rev. B: Condens. Matter Mater. Phys.* **1996**, *54*, 11169–11186.
- (25) Perdew, J. P.; Burke, K.; Ernzerhof, M. Generalized gradient approximation made simple. *Phys. Rev. Lett.* **1996**, *77*, 3865–3868.
- (26) Blöchl, P. E. Projector augmented-wave method. *Phys. Rev. B: Condens. Matter Mater. Phys.* **1994**, *50*, 17953–17979.
- (27) Monkhorst, H. J.; Pack, J. D. Special points for Brillouin-zone integrations. *Phys. Rev. B* **1976**, *13*, 5188–5192.
- (28) Souza, I.; Íñiguez, J.; Vanderbilt, D. First-Principles Approach to Insulators in Finite Electric Fields. *Phys. Rev. Lett.* **2002**, *89*, 117602.
- (29) Gonze, X.; Amadon, B.; Anglade, P.-M.; Beuken, J.-M.; Bottin, F.; Boulanger, P.; Bruneval, F.; Caliste, D.; Caracas, R.; Côté, M.; et al. ABINIT: First-principles approach to material and nanosystem properties. *Comput. Phys. Commun.* **2009**, *180*, 2582–2615.
- (30) Kang, J.; Lee, E.-C.; Chang, K. J. First-principles study of the structural phase transformation of hafnia under pressure. *Phys. Rev. B: Condens. Matter Mater. Phys.* **2003**, *68*, 054106.
- (31) Ruh, R.; Corfield, P. W. R. Crystal structure of monoclinic hafnia and comparison with monoclinic zirconia. *J. Am. Ceram. Soc.* **1970**, *53*, 126–129.
- (32) Zeng, Q.; Oganov, A. R.; Lyakhov, A. O.; Xie, C.; Zhang, X.; Zhang, J.; Zhu, Q.; Wei, B.; Grigorenko, I.; Zhang, L.; et al. Evolutionary search for new high-*k* dielectric materials: methodology and applications to hafnia-based oxides. *Acta Crystallogr., Sect. C: Struct. Chem.* **2014**, *70*, 76–84.
- (33) Ohtaka, O.; Yamanaka, T.; Kume, S. Synthesis and x-ray structural analysis by the rietveld method of orthorhombic hafnia. *Nippon Seramikkusu Kyokai Gakujutsu Ronbunshi* **1991**, *99*, 826–827.
- (34) Park, M. H.; Kim, H. J.; Kim, Y. J.; Lee, Y. H.; Moon, T.; Kim, K. D.; Hyun, S. D.; Fengler, F.; Schroeder, U.; Hwang, C. S. Effect of Zr content on the wake-up effect in Hf<sub>1-x</sub>Zr<sub>x</sub>O<sub>2</sub> films. *ACS Appl. Mater. Interfaces* **2016**, *8*, 15466–15475.
- (35) Starschich, S.; Menzel, S.; Böttger, U. Evidence for oxygen vacancies movement during wake-up in ferroelectric hafnium oxide. *Appl. Phys. Lett.* **2016**, *108*, 032903.
- (36) Starschich, S.; Boettger, U. An extensive study of the influence of dopants on the ferroelectric properties of HfO<sub>2</sub>. *J. Mater. Chem. C* **2017**, *5*, 333–338.
- (37) Moriwake, H.; Konishi, A.; Ogawa, T.; Fisher, C. A. J.; Kuwabara, A.; Fu, D. The electric field induced ferroelectric phase transition of AgNbO<sub>3</sub>. *J. Appl. Phys.* **2016**, *119*, 064102.